Journal of Bone and Mineral Metabolism
https://doi.org/10.1007/s00774-025-01644-5

ORIGINAL ARTICLE

The role of Tmem119 in the estrogen action on bone in mice

Akihito Nishikawa[1,2] · Naoyuki Kawao[2] · Yuya Mizukami[2] · Koji Goto[1] · Hiroshi Kaji[2]

Received: 30 March 2025 / Accepted: 11 September 2025

Abstract

Introduction Postmenopausal osteoporosis is a critical task in the clinical management of older individuals. Numerous studies have proposed various pathophysiological mechanisms for postmenopausal osteoporosis. Tmem119 is a crucial factor for osteoblastic bone formation, and we previously clarified its contribution to the bone anabolic effects of various osteotropic factors. However, the roles of Tmem119 in postmenopausal osteoporosis and the effects of estrogen on bone remain unknown. Therefore, we herein investigated the roles of Tmem119 in bilateral ovariectomized mice with or without Tmem119 deficiency and/or the administration of estrogen.

Materials and methods Wild-type and Tmem119-deficient mice underwent bilateral ovariectomy (OVX) and subcutaneous injections of 17β-estradiol for 6 weeks. We measured bone parameters in the femurs of mice using micro-computed tomography.

Results OVX reduced the uterine weight and trabecular bone parameters, which were increased by estrogen administration. Tmem119 deficiency significantly blunted estrogen-induced increases in uterine weight, trabecular bone volume, and trabecular thickness in OVX mice. Tmem119 deficiency also significantly blunted estrogen-induced increases in alkaline phosphatase activity in mouse osteoblasts.

Conclusion Our data indicated that Tmem119 is partly involved in the effects of estrogen on trabecular osteopenia induced by estrogen deficiency presumably by affecting osteoblasts in female mice.

Keywords Tmem119 · Bone · Estrogen · Osteoporosis · Osteoblast

Introduction

The decline in estrogen levels in postmenopausal women is strongly associated with aging-related bone loss and an increased risk of bone fracture [1, 2]. The cause of postmenopausal osteoporosis is an imbalance between osteoblastic bone formation and osteoclastic bone resorption, and estrogen deficiency is known to promote osteoclast activity [3, 4]. We previously reported that estrogen inhibited the formation of osteoclast-like cells stimulated by parathyroid hormone (PTH) by selectively acting on the PTH-responsive cyclic adenosine monophosphate pathway [5, 6]. A recent study demonstrated the involvement of hypoxia-inducible factor-1α in osteoclast formation in postmenopausal osteopenia in mice [7]. Estrogen-mediated epigenetic regulation has been shown to play a number of roles in the regulation of osteogenic responses by estrogen in human mesenchymal stem cells [8]. These findings suggest that numerous mechanisms are responsible for the effects of estrogen on bone and osteoporosis.

Tmem119 is a single-pass type 1a membrane protein, and we identified Tmem119 as a gene whose expression is enhanced by TGF-β-responsive Smad3 signaling with osteogenic activity based on a comprehensive gene transcriptome analysis of mouse osteoblastic cells [9]. Calabrese et al. identified Tmem119 as an important gene in osteoblast lineage cells in mice [10]. A clinical study showed that Tmem119 was one of the genes related to aging-associated osteopenia in human genome-wide association studies [11]. Based on the findings of *in vitro* studies, Tmem119 mutations have been implicated in the pathogenic mechanisms of the primary failure of eruption, a rare oral disease characterized by abnormal tooth eruption, by affecting glucose metabolism

✉ Hiroshi Kaji
hkaji@med.kindai.ac.jp

[1] Department of Orthopaedic Surgery, Faculty of Medicine, Kindai University, Osakasayama, Japan

[2] Department of Physiology and Regenerative Medicine, Faculty of Medicine, Kindai University, Osakasayama, Japan

Published online: 04 October 2025

and osteoblastic mineralization partly through activation transcription factor 4 (ATF4) [12]. We previously revealed the involvement of Tmem119 in the bone anabolic effects of PTH partly through the enhancement of osteoblastic bone formation in mice [9, 13]. Moreover, Tmem119 is related to bone morphogenetic protein (BMP) and Runx2 signaling through interactions with BMP-specific Smad1/5 and Runx2 during osteogenic differentiation in mice [14, 15]. We previously suggested that the commitment of Tmem119 in bone mass and PTH-enhanced bone formation was more pronounced in female mice than in male mice [13]. A recent study showed that ovariectomy (OVX) reduced Tmem119 mRNA levels in mouse bone marrow stromal cells [16]. However, the roles of Tmem119 in the effects of estrogen on bone and the pathogenesis of postmenopausal osteoporosis remain unknown.

Therefore, we herein investigated the roles of Tmem119 in the effects of estrogen on bone in OVX mice with Tmem119 deficiency.

Materials and methods

Animal experiments

All animal experiments were performed in accordance with the guidelines of the National Institutes of Health and the institutional rules for the use and care of laboratory animals at Kindai University. All procedures were approved by the Experimental Animal Welfare Committee of Kindai University (Permit number: KAME-2024-009).

Tmem119-deficient ($Tmem119^{-/-}$) mice were prepared as previously described [13]. $Tmem119^{-/-}$ mice were generated using CRISPR/Cas9 technology in C57BL/6J mouse embryos. Heterozygous Tmem119 mutant mice were intercrossed to obtain homozygous $Tmem119^{-/-}$ littermates. Twelve-week-old $Tmem119^{-/-}$ mice and their wild-type littermates ($Tmem119^{+/+}$) were used. Mice were divided into 5 groups: sham/control/$Tmem119^{+/+}$ ($n=7$), OVX/control/$Tmem119^{+/+}$ ($n=7$), OVX/control/$Tmem119^{-/-}$ ($n=11$), OVX/17β-estradiol/$Tmem119^{+/+}$ ($n=8$), and OVX/17β-estradiol/$Tmem119^{-/-}$ ($n=10$). At 12 weeks of age, mice were randomly assigned to undergo OVX or sham surgery. $Tmem119^{+/+}$ mice that had undergone sham surgery then received subcutaneous injections of corn oil for 6 weeks, while $Tmem119^{+/+}$ and $Tmem119^{-/-}$ mice that had undergone OVX received subcutaneous injections of corn oil for 6 weeks, and a total of five groups were established, including a group of $Tmem119^{+/+}$ and $Tmem119^{-/-}$ mice that had undergone OVX and received subcutaneous injections of 100 μg/kg 17β-estradiol (FUJIFILM, Wako Pure Chem. Osaka, Japan) dissolved in corn oil three times per week for 6 weeks. Mice were injected intraperitoneally with 20 mg/kg calcein 2 and 7 days prior to euthanasia. One day after the final injection of 17β-estradiol or corn oil, mice were euthanized by excess isoflurane. All mice were given food and water ad libitum. Room temperature was maintained at 24 ± 1 °C with a 12:12 h light/dark cycle.

Micro-computed tomography (μCT) analysis

A μCT analysis was performed according to previous studies [17] and the guidelines of the American Society for Bone and Mineral Research [18]. The distal femur was scanned using CosmoScan GXII (Rigaku Corporation, Yamanashi, Japan) with the following parameters: voxel size = 10 × 10 × 10 μm, X-ray voltage = 90 kV, X-ray tube current = 88 μA, exposure time = 4 min. Beam-hardening artifacts were reduced using a copper filter (0.06 mm) and an aluminum filter (0.5 mm). Prior to an analysis of the bone microstructure, raw images were reconstructed using CosmoScan GX image analysis software (Rigaku Corporation) with an isotropic voxel size of 5.5 μm. The microstructural parameters of the femur were evaluated using Analyze 14.0 (AnalyzeDirect, Inc., KS, USA). A 1-mm-thick region from the end of the growth plate was used in the trabecular analysis, and the following parameters were evaluated: trabecular bone mineral density (BMD), bone volume fraction (BV/TV), trabecular number (Tb.N), trabecular thickness (Tb.Th), trabecular separation (Tb.Sp), and trabecular connectivity density (Conn.D). A 1-mm-thick region of the middiaphysis of the femur was used in the analysis of cortical bone, and the following parameters were evaluated: cortical bone BMD, cortical bone area (Ct.Ar), and cortical bone thickness (Ct.Th).

Bone histomorphometry

Bone histomorphometric analysis was performed, as previously described [13]. Femurs were fixed in neutral buffered 4% paraformaldehyde at 4 °C overnight. They were then incubated in 6.8% sucrose in neutral phosphate buffer at 4 °C overnight and embedded in Technovit 8100 (Heraeus Kulzer, Wehrheim, Germany). Five-micrometer-thick undecalcified sections were prepared. To assess the mineral apposition rate (MAR) and bone formation rate/bone surface (BFR/BS), the region of interest was defined as a 1-mm region from the end of the growth plate, excluding the primary spongiosa of the femur.

Immunohistochemistry

Immunohistochemical analysis was performed, as previously described [17]. Femurs were fixed in neutral buffered 4% paraformaldehyde at 4 °C overnight. They were then demineralized in a 22.5% formic acid and 340 mM sodium citrate

solution at 4 °C for 24 h, and embedded in paraffin. Four-micrometer-thick decalcified sections were prepared. The sections were incubated with the anti-tartrate-resistant acid phosphatase (TRAP) antibody (Cat. No. sc-30833, Santa Cruz Biotechnology, Santa Cruz, CA, USA) at a dilution of 1:100 or the anti-ALP antibody (Cat. No. PAB12279, Abnova, Taipei, Taiwan) at a dilution of 1:200, and then incubated with appropriate secondary antibodies. Immunopositive signals were detected using the tyramide signal amplification system (PerkinElmer, Waltham, MS, USA), and distal metaphyseal regions of the femurs were photographed under a fluorescence microscope (BZ-810, Keyence, Osaka, Japan) after 4′,6-diamidino-2-phenylindole (DAPI) staining. The numbers of TRAP-positive multinuclear cells (MNCs) with three or more nuclei and ALP-positive cells at the bone surface were measured using ImageJ.

Quantitative real-time polymerase chain reaction (PCR)

Total RNA was isolated from cells using an RNeasy Mini Kit (Qiagen, Hilden, Germany), as previously described [19]. Reverse transcription was performed using a High-Capacity cDNA Reverse Transcription Kit (Applied Biosystems, Foster city, CA, USA). The incorporation of SYBR Green into double-stranded DNA, which was performed using a QuantStudio 7 Flex Real-Time PCR System (Applied Biosystems), was assessed by quantitative real-time PCR. Each PCR primer is shown in Table 1. The specific mRNA amplification of the target was measured as the Ct value, which was followed by normalization with the 18S rRNA level.

Preparation of primary osteoblasts

Calvarial osteoblasts were obtained from Tmem119$^{+/+}$ and Tmem119$^{-/-}$ mice according to a previously described method [13]. Briefly, after 3-day-old female mice were euthanized with excess isoflurane, the calvaria was removed and digested four times with 1 mg/ml collagenase and 0.25% trypsin at 37 °C for 20 min. Cells were collected from the second, third, and fourth digestions and grown in Minimum Essential Medium Alpha Modification (α-MEM, Gibco, Grand Island, NY, USA) with 10% fetal bovine serum (FBS) and 1% penicillin/streptomycin.

Alkaline phosphatase (ALP) activity

ALP activity in osteoblasts was analyzed, as previously described [13]. ALP activity was assessed using a Lab assay ALP kit (FUJIFILM, Wako Pure Chem.), according to the manufacturer's instructions. Absorbance was measured at 405 nm using a microplate reader and normalized to the total protein content.

Table 1 Primers used for real-time PCR experiments

Gene		Primer sequence
Tmem119	Forward	5′-CCTACTCTGTGTCACTCCCG-3′
	Reverse	5′-CACGTACTGCCGGAAGAAATC-3′
Osterix	Forward	5′-AGCGACCACTTGAGCAAACAT-3′
	Reverse	5′-GCGGCTGATTGGCTTCTTCT-3′
ALP	Forward	5′-ATCTTTGGTCTGGCTCCCATG-3′
	Reverse	5′-TTTCCCGTTCACCGTCCAC-3′
Osteocalcin	Forward	5′-CCTGAGTCTGACAAAGCCTTCA-3′
	Reverse	5′-GCCGGAGTCTGTTCACTACCTT-3′
TRAP	Forward	5′-CAGCTGTCCTGGCTCAAAA-3′
	Reverse	5′-ACATAGCCCACACCGTTCTC-3′
Cathepsin K	Forward	5′-GAGGGCCAACTCAAGAAGAA-3′
	Reverse	5′-GCCGTGGCGTTATACATACA-3′
RANKL	Forward	5′-CACAGCGCTTCTCAGGAGCT-3′
	Reverse	5′-CATCCAACCATGAGCCTTCC-3′
OPG	Forward	5′-AGTCCGTGAAGCAGGAGT-3′
	Reverse	5′-CCATCTGGACATTTTTTGCAAA-3′
18S rRNA	Forward	5′-CGGCTACCACATCCAAGGAA-3′
	Reverse	5′-GCTGGAATTACCGCGGCT-3′

ALP alkaline phosphatase, *TRAP* tartrate-resistant acid phosphatase, *RANKL* receptor activator of nuclear factor κB ligand, *OPG* osteoprotegerin

Osteoclast formation

Osteoclast formation in mouse bone marrow cells was analyzed, as previously described [13]. Femurs were removed from 12-week-old female Tmem119$^{+/+}$ and Tmem119$^{-/-}$ mice, and adhering tissue was cleaned off. The bone ends were cut and the marrow cavity was flushed out with 1 ml α-MEM using a 24G needle. Unfractionated whole bone marrow cells were seeded in a 96-well plate (5.0×10^4 cells/well) and cultured in 150 µl α-MEM with 10% FBS and 50 ng/ml macrophage colony-stimulating factor (M-CSF) at 37 °C for 3 days without a medium change. Osteoclast formation in 150 µl α-MEM with 10% FBS, 50 ng/ml M-CSF, and 100 ng/ml receptor activator of nuclear factor-κB ligand (RANKL) in the presence or absence of 10^{-8} M 17β-estradiol was continued at 37 °C for a further 4 days. Osteoclasts were detected using a TRAP staining kit (FUJIFILM Wako Pure Chem). The number of TRAP-positive MNCs with three or more nuclei was counted in each well.

Statistical analysis

Data are expressed as the mean with the standard error of the mean (SEM). The significance of differences was evaluated

using the Mann–Whitney *U* test for comparisons of 2 groups and a two-way analysis of variance (ANOVA) followed by the Tukey–Kramer test for multiple comparisons. The significance level was set at $P < 0.05$. All statistical analyses were performed using GraphPad PRISM 7.01 software.

Results

Effects of Tmem119 deficiency on estrogen-induced changes in body weight, food intake, and visceral white adipose tissue and uterine tissue weights

Tmem119 deficiency significantly reduced body weight in female mice, but did not affect food intake or visceral white adipose tissue or uterine weights (Fig. S1). Body weight was significantly lower in OVX Tmem119$^{-/-}$ mice than in OVX Tmem119$^{+/+}$ mice with or without the administration of 17β-estradiol (Fig. 1A), while Tmem119 deficiency did not affect food intake with or without OVX and/or the administration of 17β-estradiol (Fig. 1B). The administration of 17β-estradiol significantly reduced OVX-induced increases in visceral white adipose tissue weights in Tmem119$^{+/+}$ mice, while Tmem119 deficiency did not affect visceral white adipose tissue weights with or without OVX and/or the administration of 17β-estradiol (Fig. 1C). Uterine weights significantly decreased after OVX in Tmem119$^{+/+}$ mice, which was significantly increased by the administration of 17β-estradiol (Fig. 1D). Tmem119 deficiency significantly blunted 17β-estradiol-induced increases in uterine weights in OVX mice (Fig. 1D).

Effects of Tmem119 deficiency on estrogen-induced changes in trabecular bone parameters in femurs

Tmem119 deficiency significantly reduced BV/TV, Tb.N, and cortical BMD in the femurs of mice, but did not affect trabecular BMD, Tb.Th, Tb.Sp, Conn.D, Ct.Ar, or Ct.Th (Fig. S2), which were compatible with our previous study [13]. OVX significantly reduced trabecular BMD, BV/TV, Tb.N, and Conn.D, but increased Tb.Sp in Tmem119$^{+/+}$ mice, while the administration of 17β-estradiol significantly increased trabecular BMD, BV/TV, Tb.N, Tb.Th, and Conn.D decreased by OVX, but suppressed

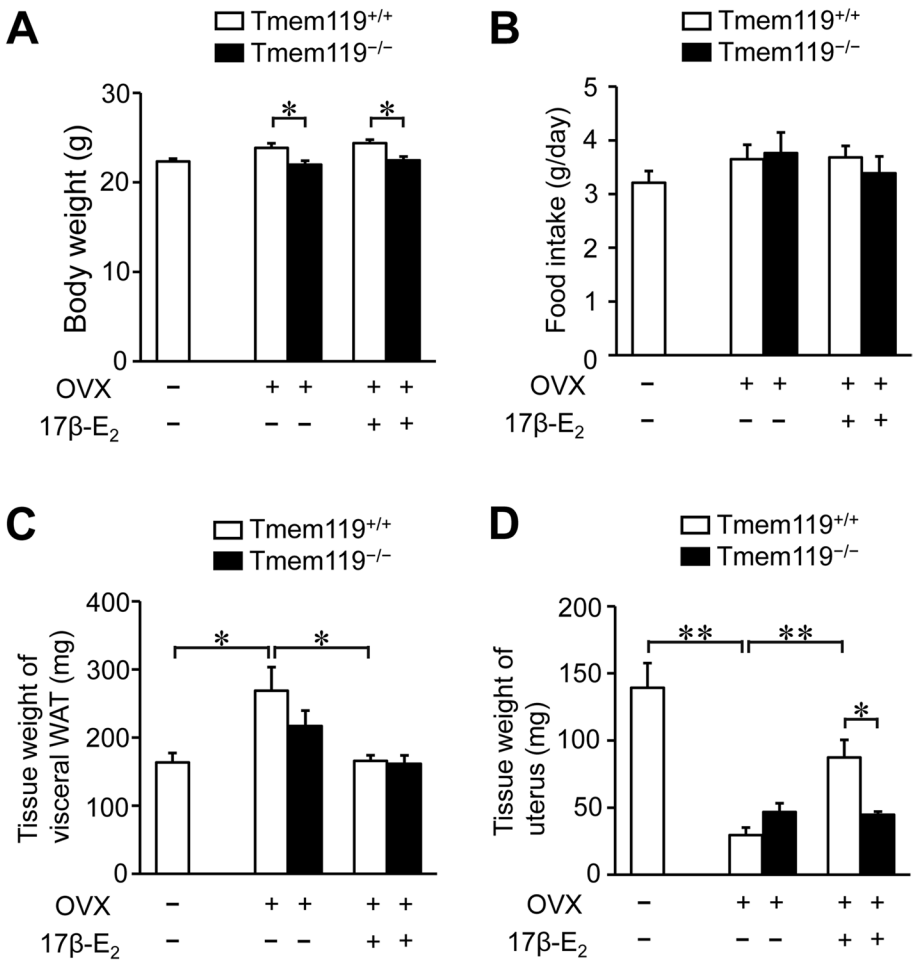

Fig. 1 Effects of Tmem119 deficiency in OVX mice treated with or without estrogen. **A** Data on body weights in Tmem119$^{+/+}$ and Tmem119$^{-/-}$ mice treated with or without 17β-estradiol (E_2). Body weight was measured 6 weeks after the first administration of 17β-E_2 or corn oil. **B** Data on food intake in Tmem119$^{+/+}$ and Tmem119$^{-/-}$ mice treated with or without 17β-E_2. Food intake was measured for 3 days on days 40–42 after OVX or the sham surgery as a representative of average daily food intake. **C**, **D** The visceral white adipose tissue (WAT) and uterus of Tmem119$^{+/+}$ and Tmem119$^{-/-}$ mice were weighed 6 weeks after OVX or the sham surgery. Data represent the mean ± SEM ($n = 7$ mice in the sham/control/Tmem119$^{+/+}$ and OVX/control/Tmem119$^{+/+}$ groups, $n = 11$ mice in the OVX/control/Tmem119$^{-/-}$ group, $n = 8$ mice in the OVX/17β-E_2/Tmem119$^{+/+}$ group, and $n = 10$ mice in the OVX/17β-E_2/Tmem119$^{-/-}$ group). *$P < 0.05$, **$P < 0.01$

Tb.Sp enhanced by OVX in Tmem119$^{+/+}$ mice (Fig. 2). Tmem119 deficiency significantly blunted 17β-estradiol-induced increases in BV/TV and Tb.Th (Fig. 2). On the other hand, OVX did not affect cortical BMD, Ct.Ar, or Ct.Th in Tmem119$^{+/+}$ mice, whereas the administration of 17β-estradiol significantly increased these cortical parameters in Tmem119$^{+/+}$ mice with OVX (Fig. 3). Tmem119 deficiency did not affect cortical BMD, Ct.Ar, or Ct.Th with or without OVX and/or the administration of 17β-estradiol (Fig. 3).

Effects of Tmem119 deficiency on estrogen-induced changes in bone histomorphometric parameters

OVX did not affect MAR or BFR/BS in the femurs of Tmem119$^{+/+}$ mice (Fig. 4A). The administration of 17β-estradiol significantly increased MAR and BFR/BS in Tmem119$^{+/+}$ mice with OVX (Fig. 4A). Tmem119 deficiency significantly decreased 17β-estradiol-induced increases in MAR and BFR/BS in OVX mice (Fig. 4A). Moreover, OVX significantly increased the number of TRAP-positive MNCs at the bone surface in Tmem119$^{+/+}$ mice, which had been significantly decreased by the

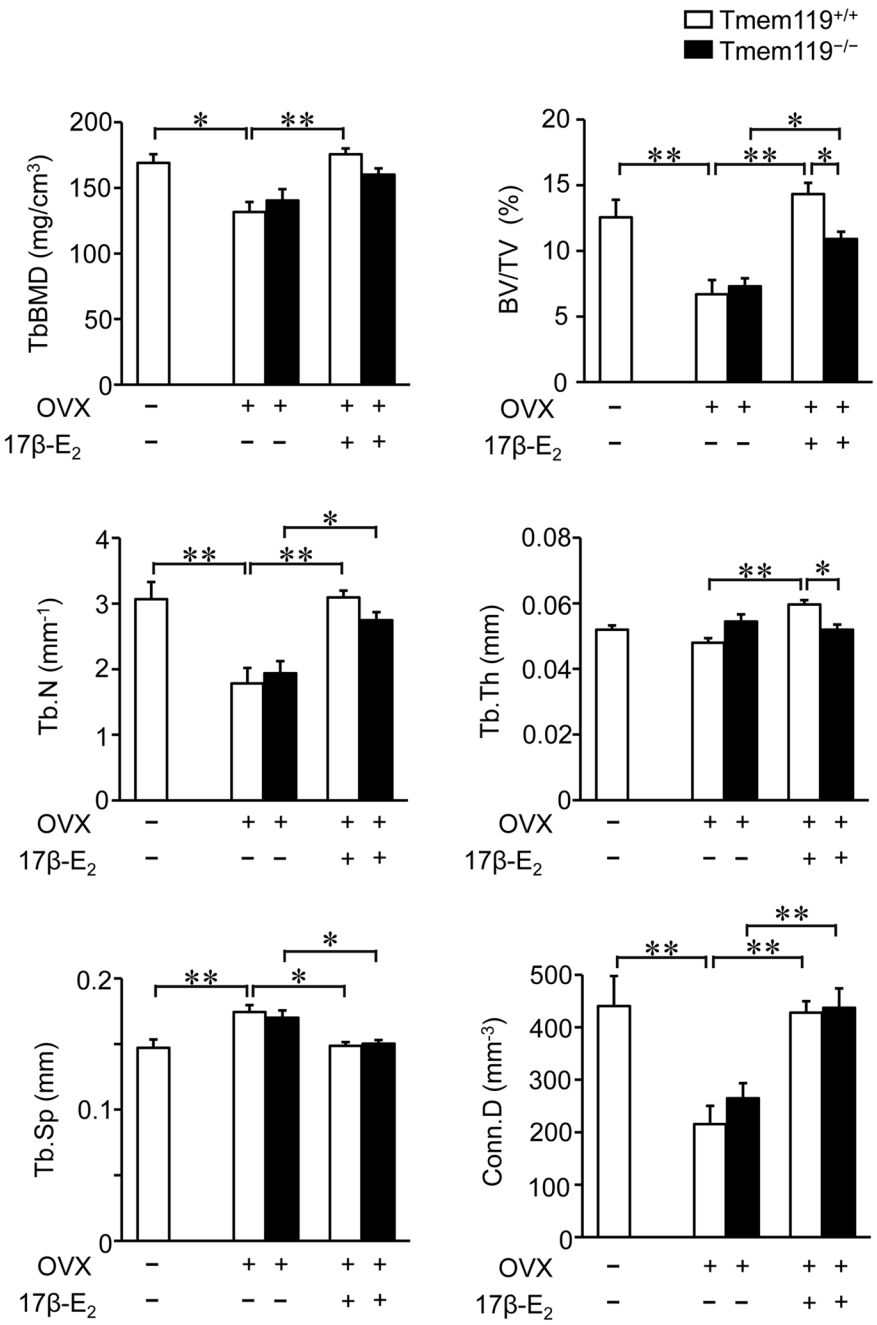

Fig. 2 Effects of Tmem119 deficiency on trabecular bone in femurs of OVX mice treated with or without estrogen. Trabecular BMD (TbBMD), BV/TV, Tb.N, Tb.Th, Tb.Sp, and Conn.D in the femurs of Tmem119$^{+/+}$ and Tmem119$^{-/-}$ mice were assessed by μCT 6 weeks after OVX or the sham surgery. Data represent the mean ± SEM ($n = 7$ mice in the sham/control/Tmem119$^{+/+}$ and OVX/control/Tmem119$^{+/+}$ groups, $n = 11$ mice in the OVX/control/Tmem119$^{-/-}$ group, $n = 8$ mice in the OVX/17β-estradiol (E_2)/Tmem119$^{+/+}$ group, and $n = 10$ mice in the OVX/17β-E_2/Tmem119$^{-/-}$ group). $^*P < 0.05$, $^{**}P < 0.01$

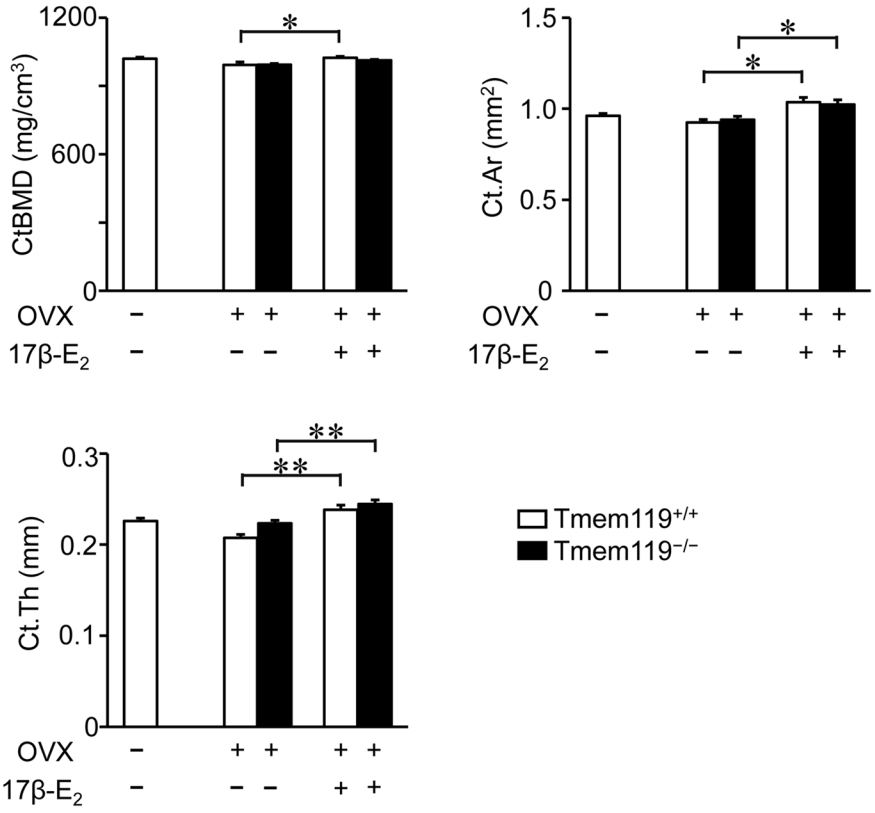

Fig. 3 Effects of Tmem119 deficiency on cortical bone in femurs of OVX mice treated with or without estrogen. Cortical BMD (CtBMD), cortical area (Ct.Ar), and cortical thickness (Ct.Th) at the femurs of Tmem119$^{+/+}$ and Tmem119$^{-/-}$ mice were assessed by μCT 6 weeks after OVX or the sham surgery. Data represent the mean ± SEM ($n = 7$ mice in the sham/control/Tmem119$^{+/+}$ and OVX/control/Tmem119$^{+/+}$ groups, $n = 11$ mice in the OVX/control/Tmem119$^{-/-}$ group, $n = 8$ mice in the OVX/17β-estradiol (E_2)/Tmem119$^{+/+}$ group, and $n = 10$ mice in the OVX/17β-E_2/Tmem119$^{-/-}$ group). $^*P < 0.05$, $^{**}P < 0.01$

administration of 17β-estradiol (Fig. 4B). Tmem119 deficiency did not affect the number of TARP-positive MNCs in OVX mice with or without the administration of 17β-estradiol (Fig. 4B). Tmem119 deficiency or OVX did not affect the number of ALP-positive cells at the bone surface in mice, although 17β-estradiol tended to increase the number of ALP-positive cells without any significant statistical differences (Fig. 4C).

Effects of Tmem119 deficiency on estrogen-induced changes in mouse osteoblasts and osteoclast formation *in vitro*

17β-Estradiol enhanced the expression of Tmem119 mRNA in mouse osteoblasts (Fig. 5A). 17β-Estradiol significantly increased the mRNA levels of ALP, but not Osterix or osteocalcin, in mouse osteoblasts (Fig. 5B). Tmem119 deficiency significantly blunted 17β-estradiol-induced increases in ALP mRNA levels (Fig. 5B). Tmem119 deficiency also significantly blunted 17β-estradiol-induced increases in ALP activity in mouse osteoblasts (Fig. 5C). RANKL and M-CSF, but not 17β-estradiol, increased Tmem119 mRNA levels in mouse bone marrow cells (Fig. 6A). 17β-Estradiol significantly reduced osteoclast formation and the mRNA levels of TRAP and cathepsin K in mouse bone marrow cells (Fig. 6B, C). Tmem119 deficiency did not affect 17β-estradiol-induced changes in osteoclast formation in mouse bone marrow cells (Fig. 6B). 17β-Estradiol significantly decreased the mRNA level of RANKL, but not OPG, and the ratio of RANKL/OPG in mouse osteoblasts (Fig. 6D). Tmem119 deficiency reduced RANKL mRNA levels and the ratio of RANKL/OPG in mouse osteoblasts, but did not affect 17β-estradiol-induced reductions in these parameters (Fig. 6D).

Discussion

The present results demonstrated that Tmem119 deficiency significantly blunted the effects of estrogen on some trabecular bone parameters as well as uterine weight decreased by estrogen deficiency in mice. *In vitro* studies revealed that estrogen increased the expression of Tmem119 in mouse osteoblasts. Moreover, Tmem119 deficiency significantly blunted the effects of estrogen on ALP activity in mouse osteoblasts.

We herein showed that Tmem119 deficiency significantly blunted 17β-estradiol-induced increases in trabecular BV/TV and Tb.Th in OVX mice, indicating that Tmem119 is partly involved in the protective effects of estrogen on trabecular bone loss associated with estrogen deficiency in mice. A previous study suggested that estrogen effectively prevented osteopenia through osteogenic differentiation via the nuclear factor erythroid 2-related factor 2 (Nrf2)-mediated activation

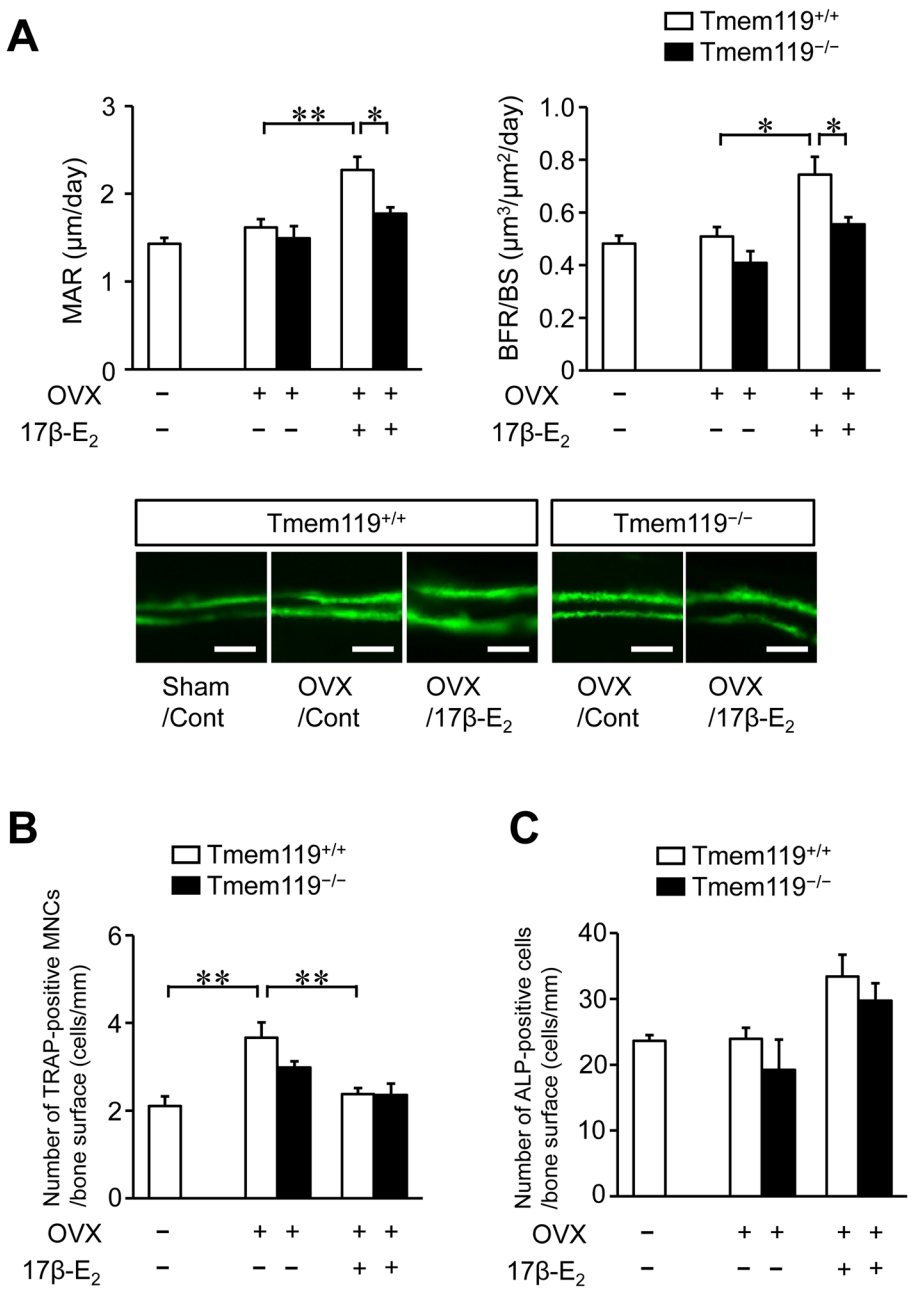

Fig. 4 Effects of Tmem119 deficiency on bone histomorphometric parameters in femurs of OVX mice treated with or without estrogen. **A** MAR and BFR/BS were examined in undecalcified sections of metaphyseal trabecular bone from the femurs of female Tmem119$^{+/+}$ and Tmem119$^{-/-}$ mice 6 weeks after OVX or the sham surgery. Scale bars indicate 25 μm. Data represent the mean ± SEM ($n = 7$ mice in the sham/control/Tmem119$^{+/+}$ and OVX/control/Tmem119$^{+/+}$ groups, $n = 11$ mice in the OVX/control/Tmem119$^{-/-}$ group, $n = 8$ mice in the OVX/17β-estradiol (E_2)/Tmem119$^{+/+}$ group, and $n = 10$ mice in the OVX/17β-E_2/Tmem119$^{-/-}$ group). **B**, **C** TRAP (**B**) or ALP (**C**) immunostaining was performed on decalcified sections of metaphyseal trabecular bone from the femurs of female Tmem119$^{+/+}$ and Tmem119$^{-/-}$ mice 6 weeks after OVX or the sham surgery. The number of TRAP-positive multinucleated cells (MNCs) or ALP-positive cells per 1 mm of the trabecular bone surface was counted. Data represent the mean ± SEM ($n = 7$ mice in the sham/control/Tmem119$^{+/+}$ and OVX/control/Tmem119$^{+/+}$ groups, $n = 6$ mice in the OVX/control/Tmem119$^{-/-}$ group, OVX/17β-E_2/Tmem119$^{+/+}$ group, and OVX/17β-E_2/Tmem119$^{-/-}$ group). $^{*}P < 0.05$, $^{**}P < 0.01$

of antioxidant signaling in mice [16]. The findings obtained showed that OVX or Nrf2 deficiency decreased Tmem119 mRNA levels in mouse bone marrow stromal cells, and the Nrf2-binding site was present in the promoter region of Tmem119, suggesting that estrogen protects against osteoporosis through Nrf2-mediated antioxidant signaling and Tmem119 expression in mice. Numerous studies have indicated the importance of Tmem119 for osteoblastic bone formation [9, 12–15]. Therefore, Tmem119 may be crucial for estrogen-deficient osteoporosis.

Estrogen-deficient osteoporosis is more pronounced in trabecular bone than in cortical bone. In our previous study, Tmem119 deficiency seemed to reduce both trabecular bone volume and cortical BMD in female mice, and the involvement of Tmem119 in the effects of PTH on bone were more prominent in trabecular bone [13]. In the present study, Tmem119 deficiency significantly blunted 17β-estradiol-induced increases in trabecular BV/TV and Tb.Th in OVX mice, but did not affect cortical BMD, Ct.Ar, or Ct.Th with or without OVX and/or the administration of 17β-estradiol. These results suggest that the contribution of Tmem119 to osteopenia was more pronounced in trabecular bone than in cortical bone in mice, which is compatible with the dominant effects of estrogen on trabecular bone. However, the

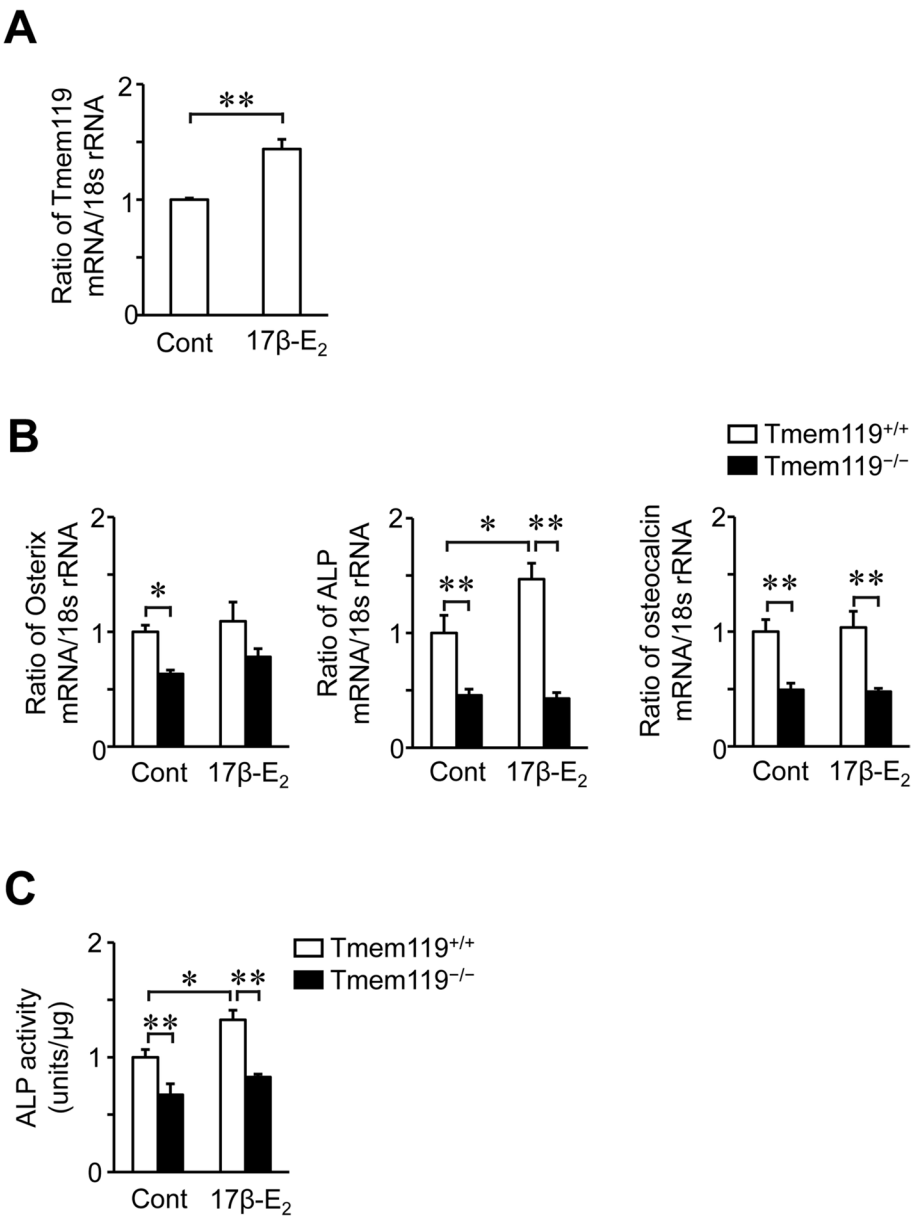

Fig. 5 Effects of Tmem119 deficiency on mouse primary osteoblasts treated with or without estrogen. **A** Osteoblasts were obtained from female Tmem119$^{+/+}$ mice. Total RNA was extracted from confluent osteoblasts treated with or without 10^{-8} M 17β-estradiol (E_2) for 24 h. A real-time PCR analysis of Tmem119 and 18S rRNA was performed. Data are expressed relative to 18S rRNA levels. Data represent the mean ± SEM. $n = 5$ in each group. **B** Osteoblasts were obtained from female Tmem119$^{+/+}$ and Tmem119$^{-/-}$ mice. Total RNA was extracted from confluent osteoblasts treated with or without 10^{-8} M 17β-E_2 for 24 h. A real-time PCR analysis of Osterix, ALP, osteocalcin, and 18S rRNA was performed. Data are expressed relative to 18S rRNA levels. Data represent the mean ± SEM. $n = 5$ in each group. **C** ALP activity was measured in confluent mouse osteoblasts cultured with or without 10^{-8} M 17β-E_2 for 48 h. Data represent the mean ± SEM. $n = 5$ in each group. $^{*}P < 0.05$, $^{**}P < 0.01$

effects of Tmem119 deficiency on estrogen-induced changes in trabecular BMD, Tb.N, Tb.Sp, and Conn.D in OVX mice were not significant in the present study. Therefore, the involvement of Tmem119 in the effects of estrogen may differ depending on the bone region and microarchitecture.

Our previous findings indicated that Tmem119 enhanced osteoblastic bone formation by enhancing Runx2, Osterix, ALP, osteocalcin, and canonical Wnt-β-catenin signaling in mice [9, 13, 14]. Moreover, Nrf2, ATF4, and BMP pathway may be related to the effects of Tmem119 in osteogenic differentiation [14–16]. Collectively, these findings suggest that Tmem119 plays a more important role in osteoblastic bone formation than in osteoclastic bone resorption. The present study showed that Tmem119 deficiency significantly blunted estrogen-induced increases in ALP activity in mouse osteoblasts. Moreover, estrogen enhanced Tmem119 expression in mouse osteoblasts. However, Tmem119 deficiency did not affect osteoclast formation or the expressions of TRAP and cathepsin K suppressed by estrogen in mouse bone marrow cells in our data. In addition, Tmem119 deficiency did not affect the ratio of RANKL/OPG decreased by estrogen in mouse osteoblasts. Therefore, Tmem119 may be involved in the effects of estrogen on osteopenia induced by estrogen deficiency presumably by affecting the influences of estrogen on osteoblasts in mice.

Due to their tissue-selective specificities, selective estrogen receptor modulators are used to treat postmenopausal osteoporosis and breast cancer [20]. Although Tmem119 is widely expressed in various tissues, its role in mediating estrogen's effects on bone suggests that it may mediate

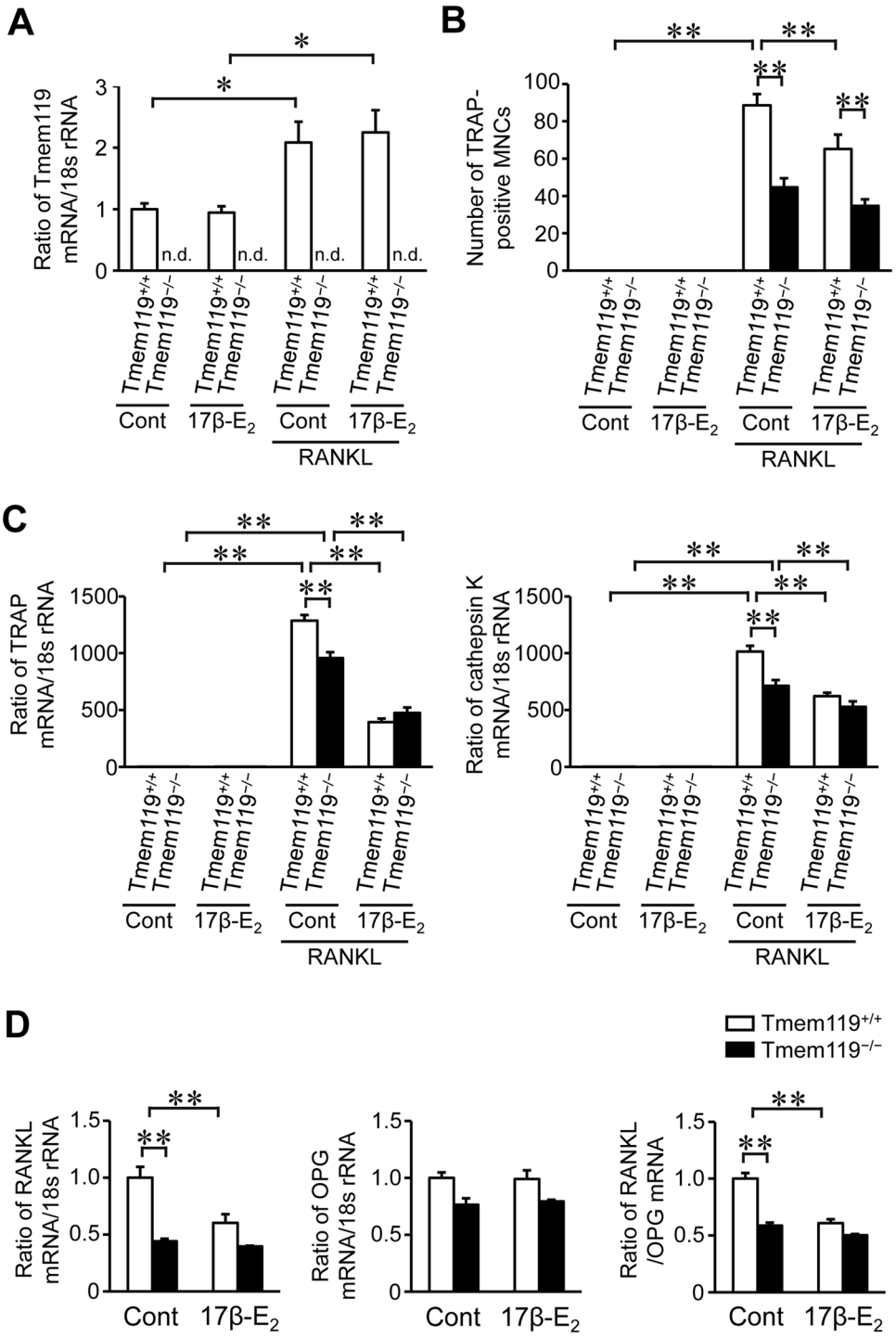

Fig. 6 Effects of Tmem119 deficiency on osteoclast formation in mouse bone marrow cells treated with or without estrogen. **A**–**C** Mouse bone marrow cells were pre-cultured with 50 ng/ml M-CSF for 3 days, and further cultured with 50 ng/ml M-CSF and 100 ng/ml RANKL in the presence or absence of 10^{-8} M 17β-estradiol (E_2) for additional 4 days. Total RNA was extracted from mouse bone marrow cells and a real-time PCR analysis of Tmem119, TRAP, cathepsin K, and 18S rRNA was performed (**A**, **C**). The number of TRAP-positive multinucleated cells (MNCs) was counted in each well (**B**). **D** Total RNA was extracted from confluent osteoblasts treated with or without 10^{-8} M 17β-E_2 for 24 h. A real-time PCR analysis of RANKL, osteoprotegerin (OPG), and 18S rRNA was performed. Data are expressed relative to 18S rRNA levels. Data represent the mean ± SEM. $n = 4$ (**A**, **C**), 6 (**B**), and 5 (**D**) in each group. $^{*}P < 0.05$, $^{**}P < 0.01$

estrogen action in a tissue-selective manner [21]. The present study showed that Tmem119 deficiency blunted estrogen-induced increases in uterine weight and trabecular bone mass, but did not affect estrogen-induced reductions in visceral adipose tissue weights in OVX mice. These results suggest that Tmem119 is involved in the effects of estrogen on both bone and uterine tissue, but not adipose tissue. However, the effects of estrogen may not be estrogen-specific effects on adipose tissue, but the secondary effects of estrogen mediated through other metabolic effects. In addition, Tmem119 deficiency slightly but significantly reduced BV/TV, Tb.N, and cortical BMD at femurs of mice without OVX, although it did not affect MAR and BFR/BS as well as the numbers of TRAP-positive MNCs and ALP-positive cells per bone surface at the femurs of mice without OVX in our previous study with the similar experimental conditions

[13]. Therefore, we cannot rule out the possibility that the effects of Tmem119 deficiency on estrogen-induced changes in bone mass in OVX mice were not estrogen-specific.

Tmem119 is a single-pass type 1a membrane protein that has a signal peptide targeted to the endoplasmic reticulum membrane. We previously showed that Tmem119 was expressed in the cytoplasm as well as the cell membrane in mouse osteoblastic cells [9]. Moreover, we demonstrated that Tmem119 contributed to the endoplasmic reticulum stress response mediated by the BMP-2-induced PERK/eIF2α/ATF4 axis during the commitment of myoblastic cells to osteoblastic cells [15]. Collectively, these findings suggest that cytoplasmic estrogen receptors may interact with Tmem119 in the endoplasmic reticulum in the cytoplasm; however, the mechanisms by which estrogen interacts with Tmem119 for its genomic effects remain unknown.

In conclusion, the present study demonstrated that Tmem119 deficiency blunted effects of estrogen on trabecular bone loss and uterine weight in OVX mice presumably through its effects on osteoblasts. These results suggest that Tmem119 is partly involved in the pathophysiology of postmenopausal osteoporosis. Tmem119 might be some clue for the medication of postmenopausal osteoporosis.

Supplementary Information The online version contains supplementary material available at https://doi.org/10.1007/s00774-025-01644-5.

Acknowledgements This study was partly supported by a grant from The Salt Science Research Foundation, No. 23C1 to H.K., and the Grants-in-Aid for Scientific Research (C: 23K08642) to H.K. from the Ministry of Education, Culture, Sports, Science, and Technology of Japan.

Author contributions A.N., N.K., and H.K. contributed to the conception and design of the research. A.N., N.K., and Y.M. performed experiments. A.N., N.K., K.G., and H.K. interpreted the results of experiments. A.N. analyzed data and prepared figures. A.N. drafted the manuscript. N.K. and H.K. edited and revised the manuscript. All authors have read and agreed to the published version of the manuscript.

Funding The work of Hiroshi Kaji was funded by Salt Science Research Foundation, under Grant No. 23C1, and Ministry of Education, Culture, Sports, Science and Technology, under Grant No. 23K08642.

Declarations

Conflict of interest All authors state that they have no conflict of interest.

References

1. Khosla S, Monroe DG (2018) Regulation of bone metabolism by sex steroids. Cold Spring Harb Perspect Med 8:a031211
2. Almeida M, Laurent MR, Dubois V, Claessens F, O'Brien CA, Bouillon R, Vanderschueren D, Manolagas SC (2017) Estrogens and androgens in skeletal physiology and pathophysiology. Physiol Rev 97:135–187
3. Emmanuelle NE, Marie-Cecile V, Florence T, Jean-Francois A, Francoise L, Coralie F, Alexia V (2021) Critical role of estrogens on bone homeostasis in both male and female: from physiology to medical implications. Int J Mol Sci 22:1568
4. Manolagas SC (2010) From estrogen-centric to aging and oxidative stress: a revised perspective of the pathogenesis of osteoporosis. Endocr Rev 31:266–300
5. Kaji H, Sugimoto T, Kanatani M, Nasu M, Chihara K (1996) Estrogen blocks parathyroid hormone (PTH)-stimulated osteoclast-like cell formation by selectively affecting PTH-responsive cyclic adenosine monophosphate pathway. Endocrinology 137:2217–2224
6. Kanatani M, Sugimoto T, Takahashi Y, Kaji H, Kitazawa R, Chihara K (1998) Estrogen via the estrogen receptor blocks cAMP-mediated parathyroid hormone (PTH)-stimulated osteoclast formation. J Bone Miner Res 13:854–862
7. Meng X, Lin Z, Cao S, Janowska I, Sonomoto K, Andreev D, Katharina K, Wen J, Knaup KX, Wiesener MS, Kronke G, Rizzi M, Schett G, Bozec A (2022) Estrogen-mediated downregulation of HIF-1α signaling in B lymphocytes influences postmenopausal bone loss. Bone Res 10:15
8. Liu Z, Lee HL, Suh JS, Deng P, Lee CR, Bezouglaia O, Mirnia M, Chen V, Zhou M, Cui ZK, Kim RH, Lee M, Aghaloo T, Hong C, Wang CY (2022) The ERα/KDM6B regulatory axis modulates osteogenic differentiation in human mesenchymal stem cells. Bone Res 10:3
9. Hisa I, Inoue Y, Hendy GN, Canaff L, Kitazawa R, Kitazawa S, Komori T, Sugimoto T, Seino S, Kaji H (2011) Parathyroid hormone-responsive Smad3-related factor, Tmem119, promotes osteoblast differentiation and interacts with the bone morphogenetic protein-Runx2 pathway. J Biol Chem 286:9787–9796
10. Calabrese G, Bennett BJ, Orozco L, Kang HM, Eskin E, Dombret C, De Backer O, Lusis AJ, Farber CR (2012) Systems genetic analysis of osteoblast-lineage cells. PLoS Genet 8:e1003150
11. Doolittle M, Khosla S, Saul D (2023) Single-cell integration of BMD GWAS results prioritize candidate genes influencing age-related bone loss. JBMR Plus 7:e10795
12. Xu M, Wang D, Li K, Ma T, Wang Y, Xia B (2024) TMEM119 (c.G143A, p. S48L) mutation is involved in primary failure of eruption by attenuating glycolysis-mediated osteogenesis. Int J Mol Sci 25:2821
13. Kawao N, Matsumura D, Yamada A, Okumoto K, Ohira T, Mizukami Y, Hashimoto D, Kaji H (2024) Tmem119 is involved in bone anabolic effects of PTH through enhanced osteoblastic bone formation in mice. Bone 181:117040
14. Tanaka K, Inoue Y, Hendy GN, Canaff L, Katagiri T, Kitazawa R, Komori T, Sugimoto T, Seino S, Kaji H (2012) Interaction of Tmem119 and the bone morphogenetic protein pathway in the commitment of myoblastic into osteoblastic cells. Bone 51:158–167
15. Tanaka K, Kaji H, Yamaguchi T, Kanazawa I, Canaff L, Hendy GN, Sugimoto T (2014) Involvement of the osteoinductive factors, Tmem119 and BMP-2, and the ER stress response PERK-eIF2α-ATF4 pathway in the commitment of myoblastic into osteoblastic cells. Calcif Tissue Int 94:454–464
16. Yang R, Li J, Zhang J, Xue Q, Qin R, Wang R, Goltzman D, Miao D (2023) 17β-estradiol plays the anti-osteoporosis role via a novel ESR1-Keap1-Nrf2 axis-mediated stress response activation and Tmem119 upregulation. Free Radic Biol Med 195:231–244
17. Matsumura D, Kawao N, Yamada A, Okumoto K, Ohira T, Mizukami Y, Goto K, Kaji H (2024) Tmem119 deficiency delays bone repair in mice. Bone 186:117177
18. Bouxsein ML, Boyd SK, Christiansen BA, Guldberg RE, Jepsen KJ, Muller R (2010) Guidelines for assessment of bone

microstructure in rodents using micro-computed tomography. J Bone Miner Res 25:1468–1486
19. Kawao N, Tamura Y, Okumoto K, Yano M, Okada K, Matsuo O, Kaji H (2013) Plasminogen plays a crucial role in bone repair. J Bone Miner Res 28:1561–1574
20. Moshi MR, Nicolopoulos K, Stringer D, Ma N, Jenal M, Vreugdenburg T (2023) The clinical effectiveness of denosumab (Prolia®) for the treatment of osteoporosis in postmenopausal women, compared to bisphosphonates, selective estrogen receptor modulators (SERM), and placebo: a systematic review and network meta-analysis. Calcif Tissue Int 112:631–646
21. Herrera-Quiterio GA, Encarnacion-Guevara S (2023) The transmembrane proteins (TMEM) and their role in cell proliferation, migration, invasion, and epithelial-mesenchymal transition in cancer. Front Oncol 13:1244740